Municipal Advisory Board

Established May 1, 2008 at the University of Texas, Arlington

Design of HDPE Water Mains for the Lateral Spread Seismic Hazard

(MAB-9 2023)

First edition approved by MAB at 29th meeting in Round Rock, TX, 2022

Effective Date: February 1, 2023

FOREWORD

This paper was developed by the Municipal Advisory Board (MAB) and published with the help of the members of the Plastics Pipe Institute, Inc. (PPI).

This publication is intended as a paper for engineers, users, contractors, code officials, and other interested parties for use in the design, construction and installation of high-density polyethylene (HDPE) pressure water piping systems. The local utility or engineer may need to modify this paper to adapt the document to local conditions, operations, and practices.

This paper has been prepared by MAB members and associates as a service to the water industry. The information in this document is offered in good faith and believed to be accurate at the time of its preparation, but is offered "as is" without express or implied warranties, including WARRANTIES OF MERCHANTABILITY AND FITNESS FOR A PARTICULAR PURPOSE. Any reference to a specific manufacturer's product is merely illustrative, and not intended as an endorsement of that product. Reference to or testing of a proprietary product should not be construed as an endorsement by the MAB or PPI, which do not endorse the proprietary products or processes of any manufacturer. Users are advised to consult the manufacturer for more detailed information about the specific manufacturer's products. The information in this document is offered for consideration by industry members in fulfilling their own compliance responsibilities. MAB and the PPI assume no responsibility for compliance with applicable laws and regulations.

The MAB serves as an independent, non-commercial adviser to the Municipal & Industrial (M & I) Division of the PPI. Once adopted, MAB will consider revising this paper from time to time, in response to comments and suggestions from the users. Please send suggestions of improvements to Camille George Rubeiz, PE, F. ASCE, at crubeiz@plasticpipe.org.

ACKNOWLEDGEMENTS

The Municipal Advisory Board would like to acknowledge the excellent contributions of the MAB Task Group for developing and leading this project.

1. **Michael O'Rourke**, Prof. Emeritus Civil Engineering, Rensselaer, **TG Chair**
2. **Rob Diamond**, PE, City of Palo Alto, CA
3. **Casey Haynes**, PE, City Utilities, Springfield, MO
4. **Bill Heubach**, Seattle Public Utilities, WA
5. **Harvey Svetlik,** PE, GPPC, TX
6. **Gerry Groen,** PEng**,** Infra Pipe, ON
7. **Camille Rubeiz**, PE, Plastics Pipe Institute, TX

MAB-09: MAB Design of HDPE Water Mains for the Lateral Spread Seismic Hazard

The required wall thickness for a fully fused HDPE water main subject to an earthquake induced lateral spread is addressed in this paper. The water main is assumed to be buried via cut and cover (i.e., open cut with typical burial depths in the 2 to 15 feet range) procedures and any laterals have small diameters and do not affect the overall seismic performance of the main. The lateral spread hazard and the fault crossing hazard are the most severe seismic hazards for buried pipelines. For the lateral spread hazard, the required wall thickness is a function of site information (burial depth and unit weight of the soil), the acceptable pipe axial strain, and geometric characteristics of the hazard (amount of ground movement and length of the lateral spread zone).

SHORT SUMMARY

Simple relations are developed for the required wall thickness for a HDPE water main subject to the lateral spread seismic hazard.

KEY WORDS: seismic hazard, HDPE water mains, PGD, lateral spread.

INTRODUCTION

The two primary seismic hazards to buried pipelines are wave propagation and permanent ground deformation. Earthquakes are caused by relative movement at a fault. This movement results in waves traveling away from the fault. The traveling waves stretch and bend pipeline infrastructure at or near the ground surface and is referred to as the wave propagation (WP) hazard. The WP hazard occurs in all earthquakes and is most commonly quantified by the resulting ground strain which is proportional to the peak ground velocity and inversely proportional to the effective propagation velocity of the traveling seismic waves[1]. The WP hazard is also transitory in that after the shaking ends, the ground returns to its original pre-quake position. If the earthquake is large, it can also result in permanent offsets at the surface or movements of the ground (lateral spread hazard) both referred to as permanent ground deformation (PGD). As noted above, this addresses the lateral spread hazard. As will be shown later, the ground strains due to PGD are larger and hence more important than those due to WP.

[1] Body Waves (P and S waves) are close to being vertically incident when they arrive at the ground surface. They appear to be traveling very fast (high apparent propagation velocity). Surface waves (e.g. Rayleigh) travel nominally parallel to the horizontal pipeline (low apparent propagation velocity)

Lateral spreads can take many forms. For lateral spreading resulting in a Ridge Pattern, the PGD is characterized by a ground strain α and the length of the PGD zone L. Another common pattern is a Block Pattern in which a block of soil at length L moves uniformly downslope by an amount δ. This form of PGD is often referred to as a lateral spread when away from a free face or a landslide when at or near a free face. Figure 1 presents a sketch of both these lateral spreading related patterns of PGD.

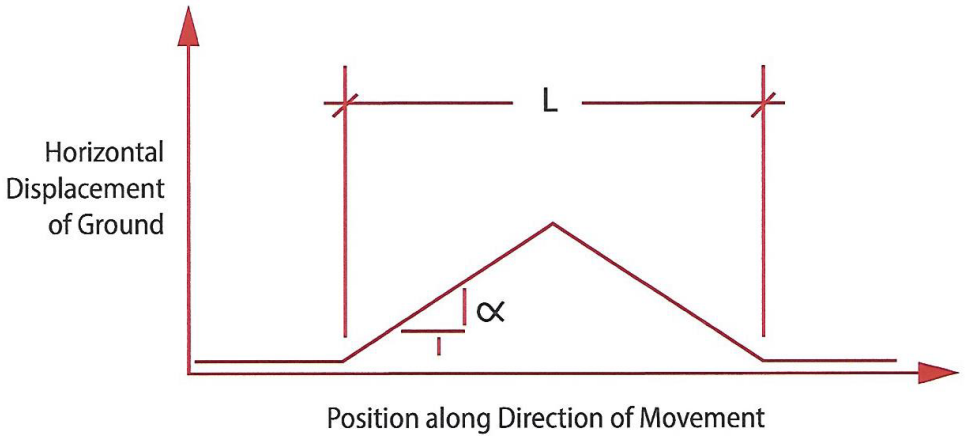

(a) Ridge Pattern

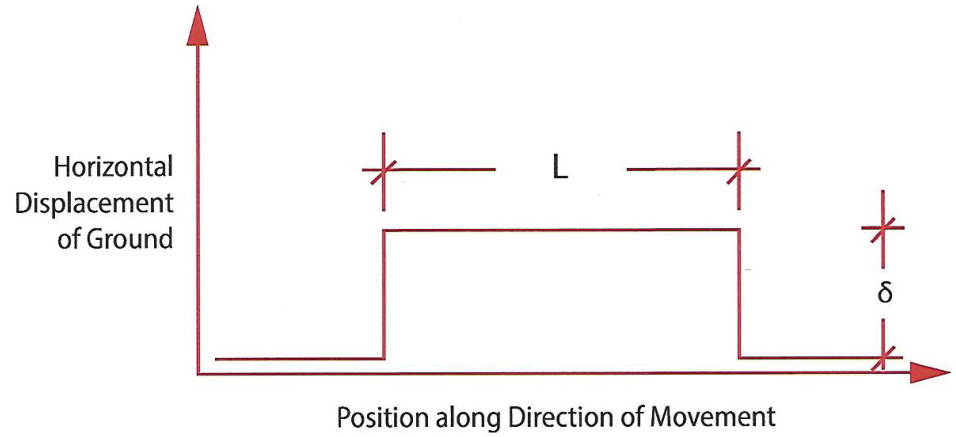

(b) Block Pattern

Figure 1 – Ridge and Block Patterns of Permanent Ground Deformation

There are some earthquakes such as the 1985 Michoacan event where all the pipeline damage in Mexico City was attributed to the WP hazard. There are other events such as the 1994 Northridge earthquake where the pipeline damage was due to both the WP and PGD hazards. In general, the WP hazard affects the whole pipeline network while the PGD hazard effects only limited portions of the network. However, in terms of the intensity of damage as measured by the repair rate (repairs per kilometer of pipe) the PGD hazard is much more intense than the WP hazard. This is due to the fact that the

PGD ground strains are generally much larger than ground strains due to WP. For example, O'Rourke et. al. (2015) investigated the inter-relationship between segmented pipe repair rates and seismic ground strain. For the 14 WP data points, the observed ground strains ranged from roughly 0.005% to 0.1% while for the 13 PGD data points, the ground strains ranged from roughly 0.05% to 5%. As one might expect, there were corresponding differences in the repair rates. For segmented pipe (primarily cast iron and PVC materials), the WP repair rates ranged from roughly 0.01 to 1.0 repairs per kilometer while the PGD repair rates ranged from roughly 2.0 to 35 repairs per kilometer. That is, one expects that if a pipeline can handle the PGD hazard, it should also be able to handle the WP hazard. As such, herein the lateral spread PGD hazard is considered while the WP hazard is not considered.

UNIFORM GROUND STRAIN PGD

For a pipeline subject to uniform ground strain such as a Ridge Pattern in Figure 1a, the orientation of the component nominally parallel to the ground strain direction (i.e., pipeline in N-S direction for ground strain in the N-S direction) produces a large axial strain in the pipeline components. It is well established that the flexural strains induced in a E-W pipeline (ground movement in the N-S direction) are comparatively small. This is consistent with the fact that it is difficult to compress a pencil (induce a given axial deformation) yet easy to bend a pencil (induce the corresponding transverse deformation via flexural strain)

The axial strain in the pipeline is a function of the length of the PGD zone and the restraint to axial movement of the pipeline provided by the soil (deep burial in stiff soil provides large soil restraint). For the Ridge Pattern in Figure 2 with downslope movement to the right, there is uniform tensile ground strain α between Points A and D, and uniform compressive ground strain α between Points D and G. For large axial resistance at the soil pipe interface (dashed line), the peak pipe tensile strain matches the ground strain between Points B and C. For small axial soil resistance (dash-dot-dash line) the peak tensile pipe strain (slope of the pipe deformation line) is less than the ground strain value. That is, for a Ridge pattern of lateral spreading, an upper bound for the axial strain in the pipeline is the ground strain value itself.

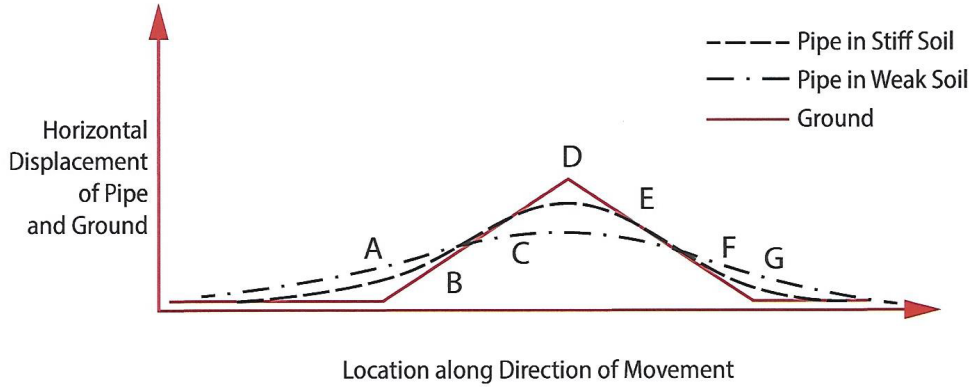

Figure 2 – Pipe Response to a Ridge Pattern of PGD

Various authors provide different estimates of ground strain. As noted above, O'Rourke et. al. (2015) presented 13 PGD ground strain data points ranging from 0.05% to 5%, while Davis et. al. (2019) present apparent ground strains of 1.2% to 2.3%. Similarly, Morimoto and Miyajima (2019) used 2.5% as the maximum value of ground strain in reclaimed ground at Port Island in the 1995 Kobe event. Appendix B of the AWWA M55 manual of Water Supply Practice provides a list of four studies with measured ground strains ranging from 0.1% to 4.5%. Omuro and Himono (2018) assert that in the Japan Water Works Association Design Code the design tensile ground strain is set at 1.2% to 2%.

Note that the pipeline composed of PE 4710 material has an elastic strain limit of about 2%, a yield strain of about 11% and an ultimate strain of about 200%. Hence a PE 4710 pipeline can accommodate expected uniform ground strains of nominally 2.5%, the JWWA design value, with a mild excursion into the inelastic range, below the yield strain and well below the ultimate strains for the material.

In summary, for a Ridge pattern of lateral spreading, the pipeline axial strain is less than or equal to the ground strain. In addition, the ground strain associated with a Ridge pattern is close in value to the elastic strain limit for HDPE pipe, below the yield strain for HDPE pipe, and well below (about a hundredth of) the ultimate strain for the HDPE material. Hence, although a Ridge pattern of lateral spreading is problematic for other pipe materials, HDPE pipe failure for this seismic hazard is unlikely and not expected. However, the Block pattern of lateral spreading, discussed below, is in general a more severe seismic hazard for buried pipelines

ABRUPT MOVEMENT PGD

The Block Pattern of PGD in Figure 1b corresponds to an abrupt uniform movement of soil downslope. Unlike the ground strains associated with a Ridge pattern, some incorrectly characterize this movement as an "equivalent" ground strain ϵ_{eq}

$$\epsilon_{eq} = \delta/L \qquad (1)$$

Unfortunately, this equivalent ground strain is neither a lower bound nor an upper bound for the induced pipeline strain.

Figure 3, shows the pipe response to a Block pattern for two different soil restraints (weak soil resistance as a dash-dot, stiff soil resistance as a dash-dash). For soil movement to the right, pipeline components have peak tensile strains at the head of the lateral spread, and peak compressive strain at the toe. However, the peak weak soil component strain (slope of line at the head and toe) is less than ϵ_{eq}, while the peak "stiff soil" component strain is greater than ϵ_{eq}. That is for a Block pattern, the ground strain is actually zero to the left of the head, zero to the right of the toe, zero between the head and the toe, and infinite at both the head and the toe. The pipe strain is less than infinity but it can be either larger or smaller than the "equivalent" ground strain given in Equation 1.

Seismic design of fully fused HDPE pipe for the lateral spread hazard involves determination of the required wall thickness. The following section provides the governing engineering relationships.

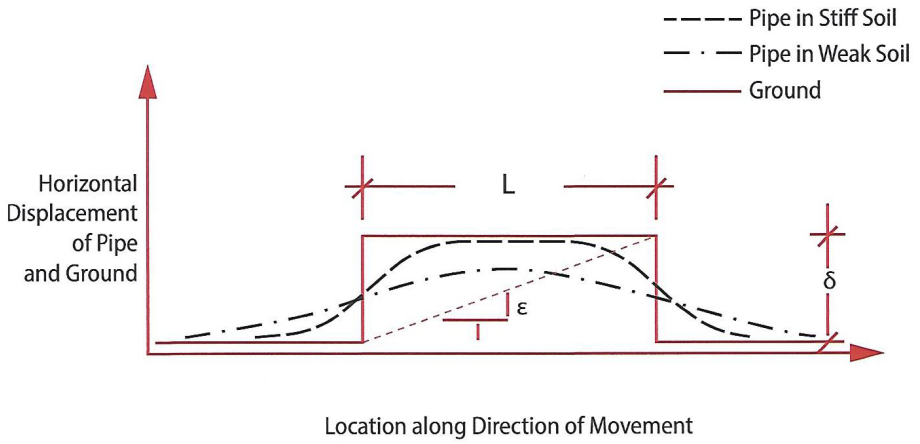

Figure 3 - -Pipe Response to a Block Pattern of PGD

REQUIRED WALL THICKNESS

O'Rourke and Nordberg (1992) have shown that for given values of δ and L, the axial strain in a fully fused or continuous buried pipeline is largest for the Block Pattern of lateral spreading. Herein we will assume the worst case (Block) pattern of lateral spreading. As noted above, a Block Pattern corresponds to a block of soil of length L moving downslope by an amount of δ. This results in "infinite" ground strain at two points, and zero ground strain elsewhere. The pipeline strains are largest for a buried pipeline nominally parallel to the direction of ground movement. This results in axial tension at the head (Point B) of the lateral spread and axial compression at the toe (Point D) as shown for Case I in Figure 4. At both the head and toe, the pipe axial strain is a maximum, less than the "infinite" ground strain but either larger or smaller than the Equivalent" ground strain in Equation 1.

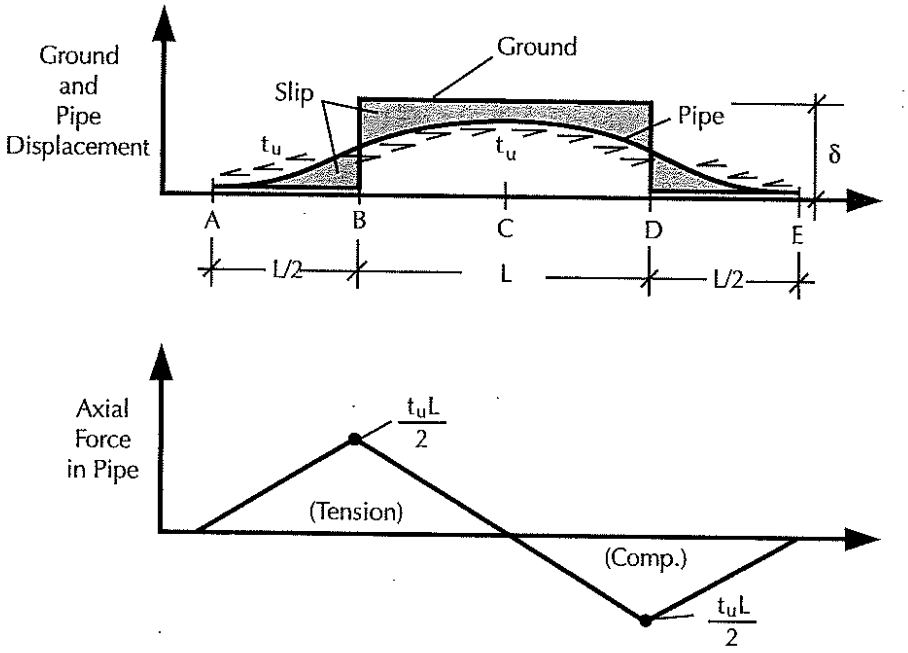

Figure 4 Ground and Pipe Displacement (upper figure), Axial Force in Pipe, (lower figure) Case I

Case I

If the length of the lateral spread is small, Case I applies as shown in Figure 4 wherein the peak pipe displacement is less than the ground displacement. The peak axial stress σ_{max} (tension at Point B, compression at Point D) is the soil friction force t_u times half the block length L, divided by the pipe cross-sectional area A

$$\sigma_{max} = \frac{t_u L}{2A} \tag{2}$$

where the soil friction force (lbs/ft) is given by

$$t_u = \pi D \gamma H \left(\frac{1+k_o}{2}\right) \mu \tag{3}$$

where D is the pipe diameter, γ is the soil unit weight taken herein somewhat conservatively to be 115 lbs/ft^3, H is the burial depth to the pipe centerline, generally in the 3 to 5 feet range, k_o is the lateral earth pressure coefficient taken herein to be 1.0, and μ is the coefficient of friction at the soil-pipe interface taken herein to be 0.25 based upon tests by Gemperline and Rinehart (2018).

Note in Figure 4 that the axial force and hence the axial stress is linear in both the head and toe regions of the lateral spread. As such the total axial displacement of the pipe is twice the displacement at the head (i.e., Point B in Figure 4). Integrating the axial strain (axial stress divided by the effective modulus of elasticity E').

$$\text{Peak Pipe Displacement} = 2\,\Delta$$

$$\Delta = \int_0^{L/2} \frac{t_u\, x}{AE'}\, dx = \frac{1}{8}\,\frac{t_u (L)^2}{AE'} \tag{4}$$

where the effective modulus of elasticity E' for HDPE pipe is a function of the allowable axial strain as shown in the Appendix.

As noted above, there are two equations of interest. From Equation 2 noting that the pipe cross-sectional area

$A = \pi\, D\, t$

$$\sigma_{max} = \frac{t_u\, L}{2\pi\, D\, t} = \frac{t_u}{2\,\pi\, D}\,\frac{L}{t} \tag{5}$$

where t is the pipe wall thickness.

Rewriting Equation 5 results in

$$\frac{L}{t} = \frac{2\,\pi\, D\, \sigma_{max}}{t_u} \tag{6}$$

while from Equation 4,

$$\text{Peak Pipe Displacement} = 2\,\Delta = \left[\frac{1}{4}\,\frac{t_u (L)^2}{\pi\, D\, t\, E'}\right]$$

or

$$\frac{L^2}{t} = \text{Peak Pipe Displacement}\ \frac{4\,\pi\, D\, E'}{t_u} \tag{7}$$

Substituting Equation (6) into Equation (7)

$$\frac{L^2}{t} = L\left(\frac{L}{t}\right) = L\left(\frac{2\,\pi\, D\, \sigma_{max}}{t_u}\right) = \text{Peak Displacement}\,\frac{4\,\pi\, D\, E'}{t_u}$$

or

$$L = \text{Peak Pipe Displacement}\left(2\,E'/\sigma_{max}\right) \tag{8}$$

However, the ratio E'/σ_{max} is a dimensionless constant which for PE 4710 material is a function of the peak strain (see Appendix).

For Case 1 the peak pipe displacement at Point C is less than the ground movement δ and hence from Equation 8

$$\text{Peak Pipe Displacement} = \frac{\sigma_{max}\, L}{2\, E'} \tag{9}$$

and

$$\delta > \text{Peak Pipe Displacement} = \frac{\sigma_{max}\, L}{2\, E'}$$

or

$$L \leq 2\, \delta\, E'/\sigma_{max} \tag{10}$$

and from Equation 5

$$t = \frac{t_u (L/2)}{\pi\, D\, \sigma_{max}} \tag{11}$$

Given the relation for t_u in Equation 3, the required wall thickness for $k_o = 1.0$ and $\mu = 0.25$ becomes

$$t = \frac{\gamma\, H\, L}{8\, \sigma_{max}} \tag{12}$$

Case II

If the length of the lateral spread zone is large, we have Case II as sketched in Figure 5 wherein the peak pipe displacement equals the ground displacement. As with Case I, the peak pipeline axial force, axial stress and axial strain still occur at the head (Point B in Figure 5) and toe (Point E in Figure 5) of the lateral spread. However, unlike Case I, the peak pipe displacement matches that for the ground between Points C and D in Figure 5. In addition, the regions of slip between the pipeline and soil are within L_e of both the head and toe of the lateral spread (between Points A and C at the head and between Points D and F at the toe).

Similar to Equation 2, for Case II the peak axial stress is at Points B and E

$$\sigma_{max} = \frac{t_u\, L_e}{A} = \frac{t_u\, L_e}{\pi\, D\, t} \tag{13}$$

or

$$\frac{L_e}{t} = \frac{\pi\, D\, \sigma_{max}}{t_u} \tag{14}$$

and the ground displacement δ can be determined by integrating the axial strain over a distance L_e

$$\delta = 2 \int_0^{L_e} \frac{t_u X}{AE'} dx = \frac{t_u (L_e)^2}{AE'} = \frac{t_u L_e^2}{\pi D t E'} \quad (15)$$

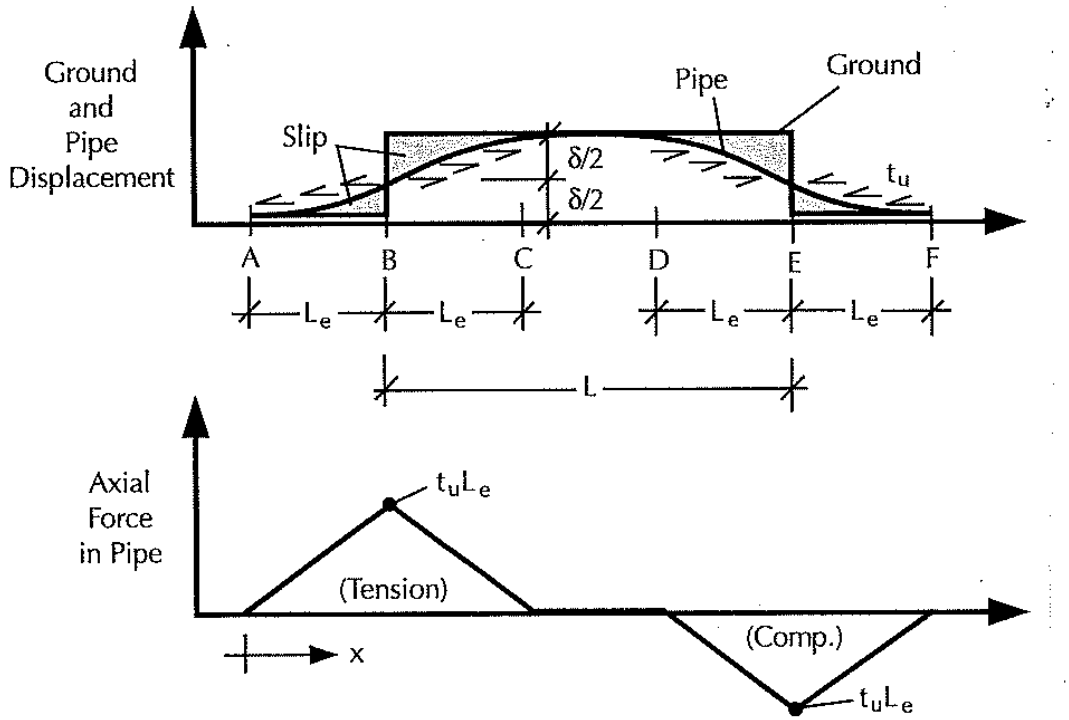

Figure 5 Ground and Pipe Displacement (upper figure), Axial Force in Pipe (lower figure) Case II

or

$$\frac{L_e^2}{t} = \frac{\pi D E' \delta}{t_u} \quad (16)$$

Substitution of Equation (14) into Equation (15) gives

$$\frac{L_e^2}{t} = L_e \left(\frac{L_e}{t}\right) = L_e \left(\frac{\pi D \sigma_{max}}{t_u}\right) = \frac{\pi D E' \delta}{t_u}$$

or

$$L_e = {E' \delta}/{\sigma_{max}} \quad (17)$$

and from Equation 13

$$t = \frac{L_e t_u}{\pi D \sigma_{max}} \tag{18}$$

where $L_e = E' \delta / \sigma_{max}$

Notice the similarity between Equations 11 and 18. The required pipe wall thickness is proportional to a length $L/2$ in Equation 11 and the length L_e in Equation 18. Both these lengths correspond to the same thing, the distance between the start of the slip between ground and pipe (Point A in both Figures 4 and 5) and the head of the lateral spread (Point B in both Figures 4 and 5). Given the relation for t_u in Equation 3, the required wall thickness, again for $k_o = 1.0$ and $\mu = 0.25$, becomes

$$t = \frac{\gamma H L_e}{4 \sigma_{max}} \tag{19}$$

Note that the required wall thickness is not a function of the pipe diameter. This results from the fact that both the lateral spread demand and the pipe capacity are both linearly proportional to the pipe diameter. Specifically, as shown in Equation 3, the soil friction force per unit length t_u is proportional to D, hence from either Equations 11 or 18, t is independent of D, the pipe diameter, as shown in Equation 12 or 19.

For Case I, the length of the lateral spread zone L is small, specifically less than $2\delta E'/\sigma_{max}$ from Equation 10, and the wall thickness is given by Equation 12. For Case II, L_e is given by Equation 17 and the wall thickness is given by Equation 19.

Figure 6 presents a simple flow chart for the determination of the required pipe wall thickness t.

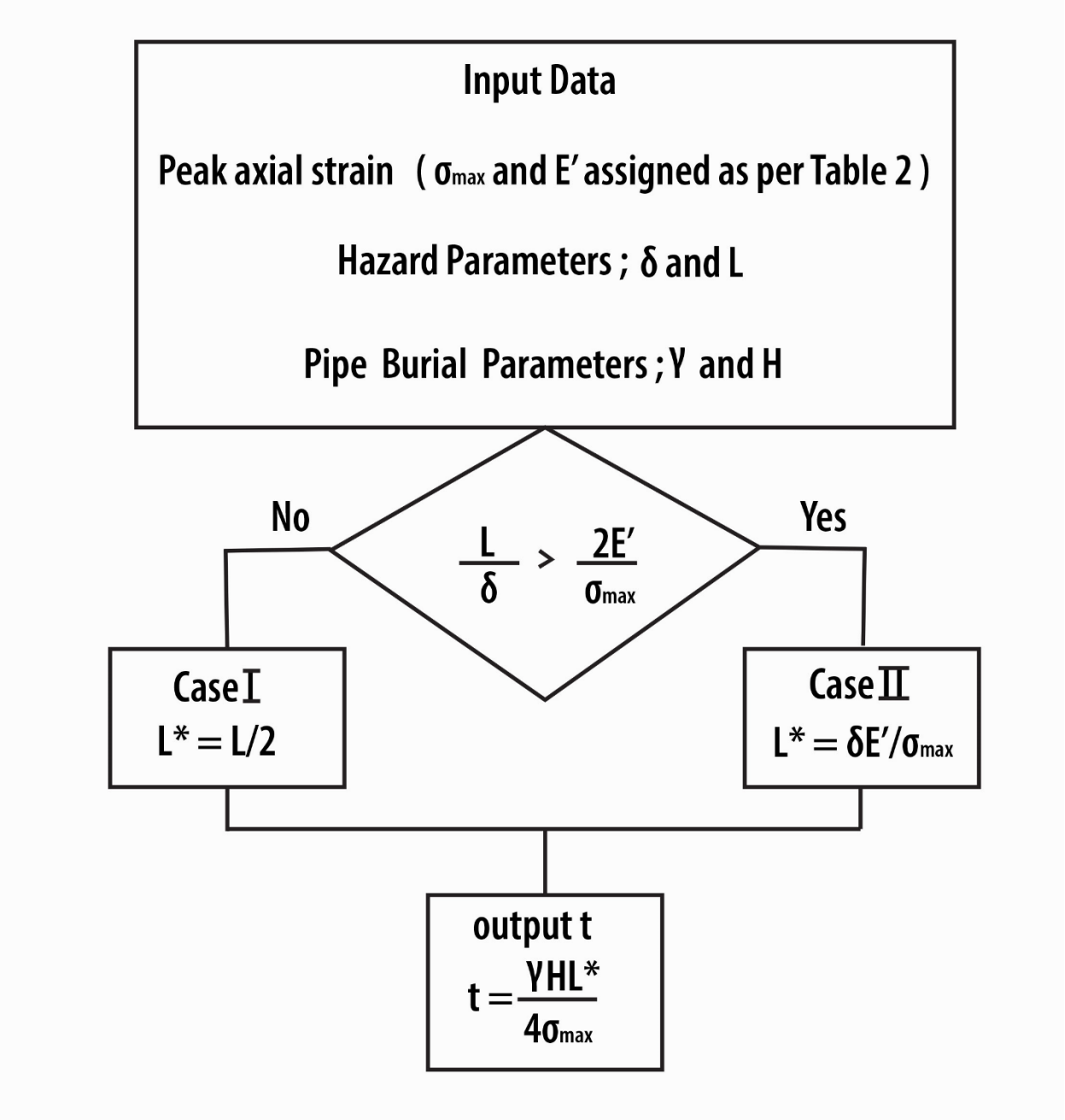

Figure 6 Flow Chart for Required Wall Thickness t

As shown in Figure 6, besides the pipe burial parameters (γ and H), users need to input information about the seismic hazard (δ and L) as well as information about the pipeline axial strain capacity. Unfortunately, local or state building codes do not specify the acceptable peak pipeline axial strain for earthquake induced lateral spreads. Hence it is the pipeline system owners/operator's, decision as to what is the acceptable peak pipeline strain. As noted above, for PE 4710 material the elastic strain limit is about 2%, the yield strain is about 11% and the ultimate strain is about 200%.

For Polyethylene PE 4710 pipe materials peak pipeline strains in the 6% to 10% range can be tolerated without fracture. It is recommended that the acceptable peak pipe strain for comparatively less important small diameter lines (diameters generally in the 4-to-12 inch range) be 8 to 10%. For more important lines (diameters generally more than 12 inches), peak pipe strains of 6 to 8% are suggested.

In relation to the seismic hazard, the two parameters used herein to characterize a lateral spread are δ, the amount of PGD movement and L, the length of the lateral spread zone. There is much more information on δ than there is on L.

GROUND DISPLACEMENT δ

Bartlett and Youd (1995) present a summary of the available relationships for the amount of ground movement δ. In particular, they mention the Hamada et. al. (1986) empirical relation for the amount of horizontal displacement as a function of the thickness of the liquefied layer and a slope. The slope value to be used is the larger of a) the slope of the bottom of the liquefied layer or the slope of the ground's top surface. Also mentioned is the Youd and Perkins (1987) Liquefaction Severity Index (LSI) in which the horizontal ground displacement is a function of the earthquake magnitude (moment magnitude) and the shortest site-to-fault distance. Finally, they cite the Ambrasey (1988) bounding relation between the moment magnitude and the furthest distance to observed liquefaction.

Bartlett and Youd (1995) then show the development of a relation for the amount of ground movement as a function of: the earthquake magnitude, M_W; the source to site distance, R; a slope factor; the thickness of the saturated layers with $(N_1)_{60} \leq 15$, T_{15}; the average fines content in T_{15}, F_{15}; and average mean grain size in T_{15}, $(D_{50})_{15}$. The slope factor for a lateral spread away from a free face is simply the ground slope, while at a free face the slope factor is proportional to the height of the free face divided by the horizontal distance to the lateral spread.

In both the 1995 version and the revised 2002 version (Youd, Hansen and Bartlett, 2002), there are seven parameters in both the free face and ground slope equations, as well as a flow chart needed for their application. Neither of the Youd relations or flow charts are presented herein since the proper application would need to be done by a Civil Engineer with a specialization in the earthquake aspects of Geotechnical Engineering.

Herein a simpler but limited method to estimate δ will be provided for typical site conditions. The typical site is assumed to be a free face with a slope factor (W) of 5%, T_{15} = 3.0 m, F_{15} = 10% and $(D_{50})_{15}$ = 0.20 mm.

Figure 7 adapted from the corresponding figure in Youd et. al. (2002) presents the predicted displacement for various values of the earthquake magnitude, M, and the horizontal site-to-source distance R. Both Youd equations were based upon a combination of observed data points from the U.S. and Japan. Although a few of the

Japanese datapoints have δ values of about 15 m, U.S. data points had δ of 4.5 m or less. Youd also cautions that δ values of 6.0 m or more are questionable and that R or R_{eq} should be no smaller than 0.5 km.

For sites in the U.S. and southern Canada, the United States Geological Survey web site https://earthquake.usgs.gov/hazards/interactive provides earthquake magnitude M_w and closest distance information. Users need to choose an edition, a site class and a spectral period. "Dynamic: Conterminous U.S. 2014 (update) (V4.2.0)" is suggested for the edition, "B/C boundary" is suggested as the default site class and Peak Ground Acceleration is suggested as the spectral period. Requesting Deaggregation provides a 3-dimensional plot of contribution to the hazard as the vertical axis and magnitude and closest distance as the two horizontal axes.

Table 1 provides the closest distance and the moment magnitude corresponding to the highest contribution for a number of U.S. and Canadian sites. Consistent with Figure 7, only events with $M_w \leq 8.0$ and distance $\leq$ 100 km are listed. The user also needs to choose a Time Horizon, (i.e., return period in years). 2475 years is the suggested value although the moment magnitude and distant are not a function of the return period value. There is a single magnitude and distance pair for most sites in Table 1. The exceptions are St. Louis, MO and others for which there is a lower magnitude event with a short distance and a higher magnitude event with a larger distance. Some sites such as Cannon Beach, OR have moment magnitudes larger than 8.0. For these sites Figure 7 does not apply and it is recommended that a seismically knowledgeable geotechnical engineer be retained to estimate the design ground displacement δ using the Youd relationship. Sites such as Cannon Beach are not included in Table 1.

Other sites such as Sacramento, CA have some contributing events with magnitudes greater than 8.0 and other contributing events with magnitude less than 8.0. For such sites, the contributing events for which Figure 7 applies (moment magnitude $\leq$ 8.0, distance $\leq$ 100 km) are listed in Table 1. The fact that there are other contributing events for which Figure 7 does not apply (e.g., the moment magnitude 9.3 event at 245 km from Sacramento) is indicated by an asterisk.

Table 1 Earthquake Magnitude and Closest Distance for Selected U.S. Cities.

City	Magnitude (M_w)	Distance (km)
Albuquerque	6.7	5
Boise	7.1	25
Charleston	7.3	5
Denver	4.8	5
Los Angeles	6.8	10
Memphis*	7.5	50
Montreal	4.8 6.2	5 25
Oakland*	7.5	5
Phoenix	6.3 6.8 7.3	25 45 65
Portland*	6.8	5
Quebec	4.8 6.8	5 45
Sacramento*	6.3 7.2 7.7	5 45 65
Salt Lake	6.8	5
San Diego	6.8	10
San Francisco	7.8	5
Seattle*	7.2	5
Springfield, MO*	4.8	5
St. Louis*	4.8 6.2	5 25
Vancouver*	7.1	5

For consistence with Figure 7, only $M_w \leq 8.0$ and Distance $\leq$ 100 km are considered. Asterix indicates contributing events above the Figure 7 limits. Also shown on the Figure B1 map in Appendix B.

LENGTH OF LATERAL SPREAD ZONE L

Available information on the length of the lateral spread zone is more limited than that for the amount of movement δ. Hamada (1986) presented the observed δ and L for 27 lateral spreads in Japan. As shown in Table 2, the L values ranged from 35 to 720 meters with a median value of 350 m. Figure 8 shows the Hamada values for δ plotted versus the Hamada values for L. Note that there is no substantial correlation between the two geometric parameters. Honegger (1994) presents a cumulative distributed function of the length of the lateral spread zone shown in Figure 9. The Honegger curve

is based upon over 150 measured lateral spread lengths from two Japanese events. Honegger contends that his values for L are reasonably consistent with expected corresponding values in North America (specifically for Vancouver B.C.) Note that for the Honegger data, the median value is about 90 m (295 ft.), the 75% below value is about 150 m (492 ft.) while the 95% below value is about 280 m (918 ft.).

Table 2 Observed Lateral Spread Displacement δ and Length of the Zone L from Hamada et. al.

Section	δ (m)	L (m)	L/δ
S-1	3.3	340	103
S-2	4.0	230	57.5
S-3	4.0	265	66.3
S-4	3.0	385	168
S-5	3.0	455	151
S-6	3.0	520	175
S-7	2.1	615	293
S-8	2.5	300	120
S-9	1.4	300	214
S-10	1.8	150	83
S-11	1.4	250	178
S-12	1.5	35	23
S-13	2.6	210	81
S-14	2.0	190	95
S-15	2.5	140	56
S-16	2.0	280	140
S-17	1.8	380	211
S-18	1.8	480	116
S-19	2.5	290	116
N-1	1.2	350	291
N-2	2.2	470	213
N-3	2.6	590	227
N-4	2.7	720	267
N-5	2.2	420	191
N-6	1.8	740	411
N-7	2.0	390	195
N-8	2.3	500	217

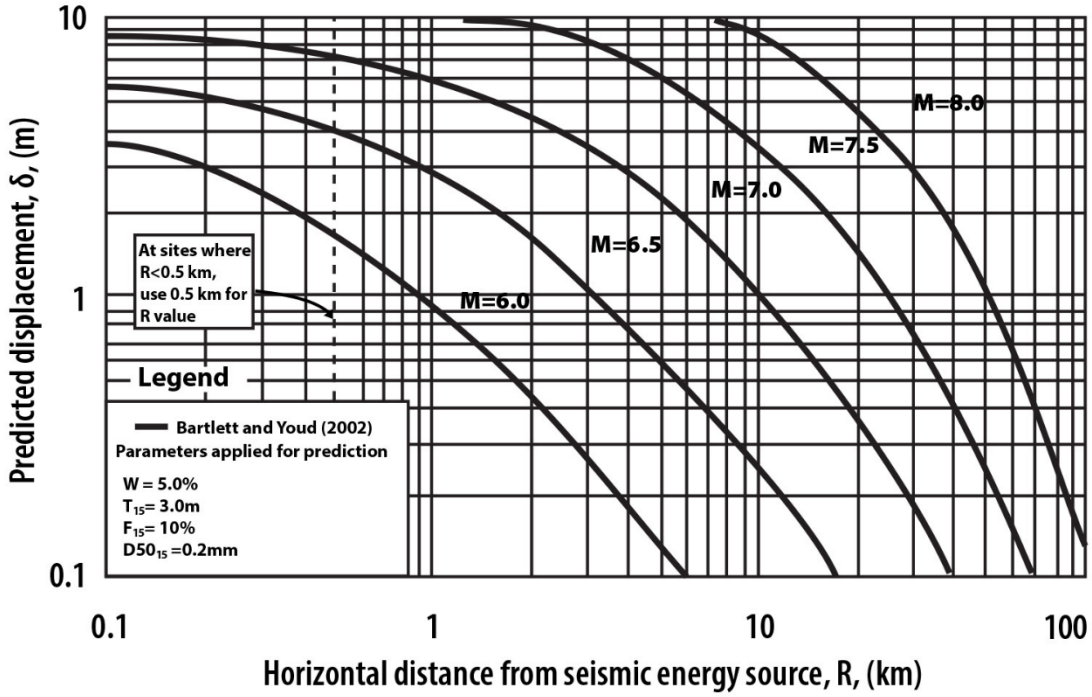

Figure 7 Youd et. al. Predicted Displacement δ as a Function of Earthquake Magnitude M and Horizontal Distance from Seismic Energy Source R

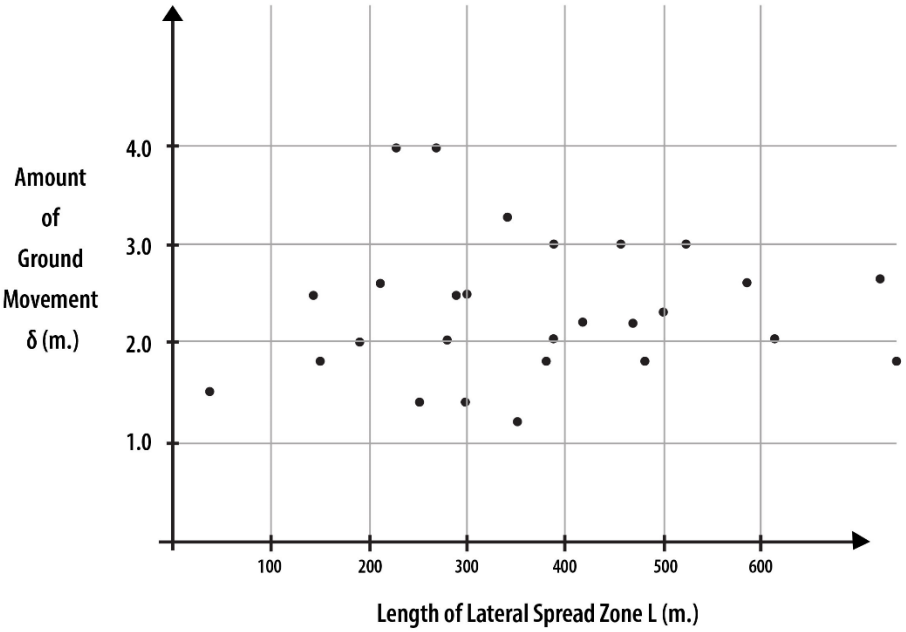

Figure 8 Scattergram of Amount of Movement δ and Length to Zone L for Hamada Data

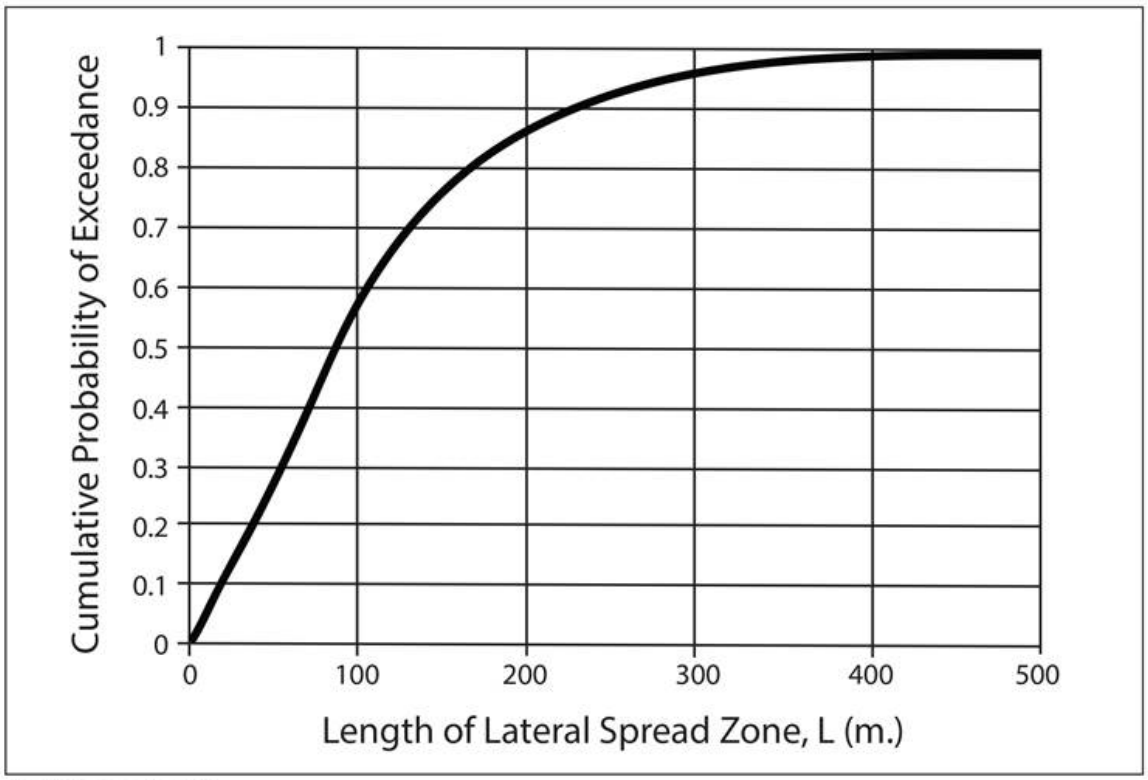

Figure 9 Cumulative Distribution Function

A project specific estimate for the length of the potential lateral spread could be determined through a geotechnical engineering study of the plan area of liquefiable soil.

As suggested in the flow chart in Figure 6, the two pipe properties needed to determine the required wall thickness are the effective modulus E´ and the peak axial stress, both of which are functions of the maximus allowable axial strain. Figure A1 in the Appendix provides the peak axial stress σ_{max} and Table A3 provides the effective modulus E´. For convenience, both parameters are summarized in Table 3. Note that the yield strain is about 8% and hence the peak stress for 8 and 10% strain are nominally the same.

Table 3 Peak Stress and Effective Modulus for Various Peak Strain Values

Peak Strain	Peak Stress (psi)	Effective Modulus (psi)	Ratio E'/σ_{max}
6%	4040	145,650	36.1
8%	4250	134,860	31.7
10%	4250	127,460	30.0

As shown in the flow chart in Figure 6, Case I applies if

$$L < 2\,\delta\,E'/\sigma_{max}$$

or

$$L/\delta < 2\;E'/\sigma_{max} \qquad (20)$$

Based upon Table 3, the inequality in Equation 20 holds for only 3 of the 27 Hamada observed lateral spreads for peak pipe strains of 8 and 10% and only 4 of the 27 for a peak strain of 6%. That is, about 89% of the Hamada lateral spreads were Case II, for which the amount of movement δ controls the pipe wall thickness, as opposed to the length of the zone L. This is fortunate since there is much more information for δ than for L.

WALL THICKNESS EVALUATION

The following is an example of the suggested determination of the required wall thickness. The site in question has a moment magnitude of 8.0 and a closest distance of 40 km from the USGS website. As such, the ground displacement from Figure 7 is δ = 2 m (6.56 ft). The length of the zone is taken to be L = 280 m (918 ft.), the 95% below value from the Honegger cumulative distribution function in Figure 9. The peak axial strain is taken to be 8%, hence from Table 3 the maximum axial stress σ_{max} = 4250 psi and the effective Elastic Modulus E´ = 134,860 psi. The HDPE pipe is buried in soil with unit weight γ = 115 lb/ft^3 and a burial depth to the center line of the pipe H = 4 feet.

The L/δ ratio is (918/6.56) = 140, while the $2E'/\sigma_{max}$ ratio is 2(134,860/4250) = 63.4. Hence as per the flow chart in Figure 6, we have Case II and $L^* = E'\delta/\sigma_{max}$ = 134,860 (6.56)/4250 = 208 ft. the required wall thickness is then $t = \gamma H L^*/4\,\sigma_{max}$ = (115 lb/ft^3)(4 ft)(208 ft)(1.0 ft/12 in)/(4(4250 lb/in^2)) = 0.47 in.

Tables 4, 5, and 6 present the required wall thickness t for peak pipe strains of 6%, 8%, and 10% and various values for the burial parameters γ and H, and for three values of the ground displacement δ. Tables 4 through 6 are for Case II, where the wall thickness is controlled by the ground displacement δ. For convenience, the corresponding minimum length of the lateral spread zone L_{min} (i.e., $L_{min} = 2\,\delta\,E'/\sigma_{max}$) is also listed. As one would expect from the flow chart in Figure 6, the required wall thickness for Case II is an increasing function of the soil unit weight γ, the burial depth H, and the ground displacement δ, and a decreasing function of the peak pipe strain.

Table 4 Required Wall Thickness t (in inches) for Case II and Peak Pipe Strain of 6%

δ	L_{min}	γ = 100 lb/ft^3			γ = 115 lb/ft^3		
(ft)	(ft)	H = 2 ft	H = 4 ft	H = 6 ft	H = 2 ft	H = 4 ft	H = 6 ft
3.28	237	0.12	0.24	0.37	0.14	0.28	0.42
6.56	473	0.24	0.49	0.73	0.28	0.56	0.84
9.85	710	0.37	0.73	1.10	0.42	0.84	1.26

Table 5 Required Wall Thickness t (in inches) for Case II and Peak Pipe Strain of 8%

δ	L_{min}	γ = 100 lb/ft^3			γ = 115 lb/ft^3		
(ft)	(ft)	H = 2 ft	H = 4 ft	H = 6 ft	H = 2 ft	H = 4 ft	H = 6 ft
3.28	208	0.10	0.20	0.31	0.12	0.23	0.35
6.56	416	0.20	0.41	0.61	0.23	0.47	0.70
9.85	625	0.31	0.61	0.92	0.35	0.70	1.06

Table 6 Required Wall Thickness t (in inches) for Case II and Peak Pipe Strain of 10%

δ	L_{min}	γ = 100 lb/ft^3			γ = 115 lb/ft^3		
(ft)	(ft)	H = 2 ft	H = 4 ft	H = 6 ft	H = 2 ft	H = 4 ft	H = 6 ft
3.28	197	0.10	0.19	0.29	0.11	0.22	0.33
6.56	393	0.19	0.39	0.58	0.22	0.44	0.67
9.85	591	0.29	0.58	0.87	0.33	0.67	1.00

As noted above, Case II for which δ controls the required wall thickness, is more common than Case I, at least for the Hamada et al. observations. For completeness Tables 7 through 9 present the required wall thickness for Case I, similar to Tables 4 through 6. For convenience the corresponding minimum ground displacement δ_{min} (i.e. $\delta_{min} = L\ \sigma_{max}/2\ E´$) is also listed. As with Case II, the required wall thickness for Case I is an increasing function of the soil unit weight γ, and the burial depth H. The Case I wall thickness is also an increasing function of the length of the zone L. The wall thickness, again for Case I, is a decreasing function of pipe strain below nominal yield at 8%. Above a peak pipe strain of 8%, the required wall thickness is constant. This seemingly odd result is due to the fact that in Case I the required wall thickness is inversely proportional to σ_{max}, which as shown in Table 3 is constant above a peak pipe strain of 8%. On the other hand, in Case II the required wall thickness is proportional to the effective modulus E´ which decreases as the peak pipe strain increases.

Table 7 Required Wall Thickness (in inches) t for Case I and Peak Pipe Strain of 6%

L	δ_{min}	γ = 100 lb/ft^3			γ = 115 lb/ft^3		
(ft)	(ft)	H = 2 ft	H = 4 ft	H = 6 ft	H = 2 ft	H = 4 ft	H = 6 ft
328	5	0.17	0.34	0.51	0.19	0.39	0.58
656	9	0.34	0.68	1.01	0.39	0.78	1.17
985	14	0.51	1.01	1.52	0.58	1.17	1.75

Table 8 Required Wall Thickness (in inches) t for Case I and Peak Pipe Strain of 8%

L	δ_{min}	γ = 100 lb/ft^3			γ = 115 lb/ft^3		
(ft)	(ft)	H = 2 ft	H = 4 ft	H = 6 ft	H = 2 ft	H = 4 ft	H = 6 ft
328	5	0.16	0.32	0.48	0.18	0.37	0.56
656	10	0.32	0.64	0.96	0.37	0.74	1.11
985	16	0.48	0.97	1.45	0.56	1.11	1.67

Table 9 Required Wall Thickness (in inches) t for Case I and Peak Pipe Strain of 10%

L	δ_{min}	γ = 100 lb/ft^3			γ = 115 lb/ft^3		
(ft)	(ft)	H = 2 ft	H = 4 ft	H = 6 ft	H = 2 ft	H = 4 ft	H = 6 ft
328	5	0.16	0.32	0.48	0.18	0.37	0.56
656	11	0.32	0.64	0.96	0.37	0.74	1.11
985	16	0.48	0.97	1.45	0.56	1.11	1.67

The diameter over wall thickness ratios (DR) for various grades of HDPE pipe (PE 4710) are shown in Table 10 along with the corresponding wall thicknesses for diameters of 8, 16, and 24 inches. For the most common case, Case II, a large ground movement displacement δ = 3.0 m (9.85 ft.) and the worst-case unit weight of soil and burial depth (γ = 115 lb/ft^2 and H = 6.0 ft.) in Tables 4 to 6, the required wall thickness t= 1.0 inch for peak pipe strain of 10% (suggested for small diameter pipe). Hence an 8-inch diameter line would require a DR of 7 (wall thickness provided of 1.23 in.). For the two larger diameters with a suggested peak pipe strain of 8%, the same conditions would require t = 1.06 inches, that is DR 13.5 for the 16-inch line and DR 21 for the 24-inch line.

Table 10 Wall Thicknesses for Various DRs and Diameters of PE 4710 pipe

Nominal DIPS Pipe Size	DR21 PC 100	DR17 PC125	DR13.5 PC160	DR11 PC200	DR9 PC250	DR7 PC335
8”	0.411”	0.507”	0.639”	0.784”	0.958”	1.232”
16”	0.762”	0.941”	1.185”	1.455”	1.778”	2.286”
24”	1.143”	1.412”	1.778”	2.182”	2.667”	3.429”

CONCLUSIONS

A procedure for calculating the required wall thickness for an HDPE water main subject to the lateral spread hazard is presented. The water main is assumed to have either no laterals or only small diameter laterals that would not significantly restrict water main movement. Separate acceptable peak pipe strains are recommended for “important” water mains (diameters greater than 12 inches) and for “less important” mains (diameters less than 12 inches). The required wall thicknesses are shown to be an increasing function of the burial depth and unit weight of backfill. Somewhat surprisingly, the required wall thickness is shown to be independent of the pipe diameter. Examples show that even for large amounts of ground movement and poor burial conditions (heavy backfill and deep burial depth) the required wall thickness is met by currently available pipe DR. This is consistent with the excellent seismic performance of HDPE pipe in past earthquakes.

Appendix A

Effective Modulus E'

Figure A1 presents the stress strain curve for a PE 4710 specimen subject to uniform axial stress as determined in an EPRI report (2008). As one might expect, the material softens with increasing axial strain. Table A1 shows the secant elastic modulus E_i at various levels of axial stress.

Table A1 Stress, Strain and Secant Modulus E_i for HDPE Material

Stress (psi)	Strain (%)	Secant Modulus E_i (psi)
1000	0.425	235,300
2000	1.06	188,700
3000	2.23	134,500
4000	5.32	75,200

The secant modulus applies for cases where the axial stress is constant along the full length of the specimen (e.g., corresponding to a specimen in a testing machine). However, as shown in Figure 4 and 5, the axial force and the axial stress in the pipe are not constant for a block pattern of lateral spread. For both Case I and II, the axial stress in the pipeline is linearly increasing or decreasing in the regions where the pipe is carrying load.

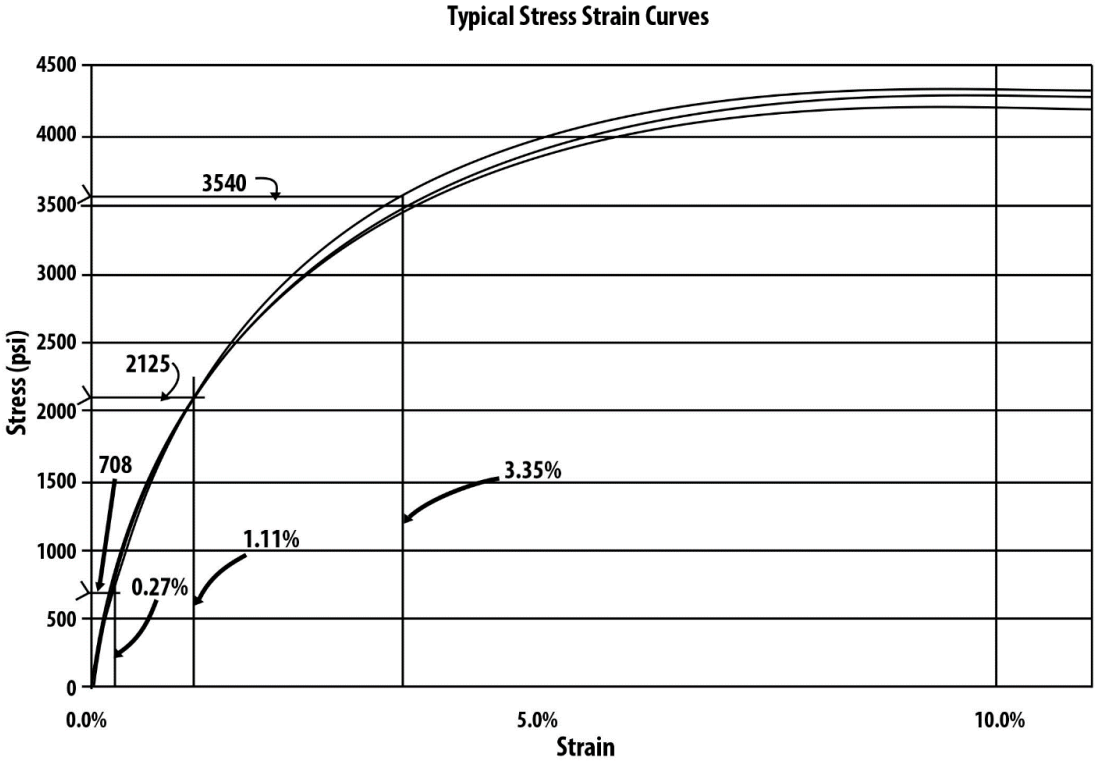

Figure A1 Stress – Strain Curve for PE 4710 Material

Also note that the peak pipe displacement plays a key role in the determination of whether Case I or Case II controls, and the corresponding required wall thickness. For a pipeline subject to a lateral spread, determination of the peak pipe displacement requires an effective modulus E' corresponding to a specimen with a linear increase in axial stress.

Consider the pipe segment between Points A and B in either Figure 4 or 5. As sketched in Figure A2, the pipe stress is a linear function of the distance from Point A. In Figure A3 the pipe segment is sub-divided into three sub-segments each with a constant pipe modulus E_i corresponding to the axial stress at the midpoint of the sub-region. The total pipe stretch Δ between Point A and B is the sum of the pipe deformations over each sub region. For sub-region 2

$$\Delta_2 = \int_{l/3}^{2l/3} \frac{t_u \, x \, dx}{AE_2} = \frac{t_u}{AE_2} \left. \frac{x^2}{2} \right|_{l/3}^{2l/3} = \frac{t_u}{2AE_2} \left(\frac{l}{3}\right)^2 [2^2 - 1]$$

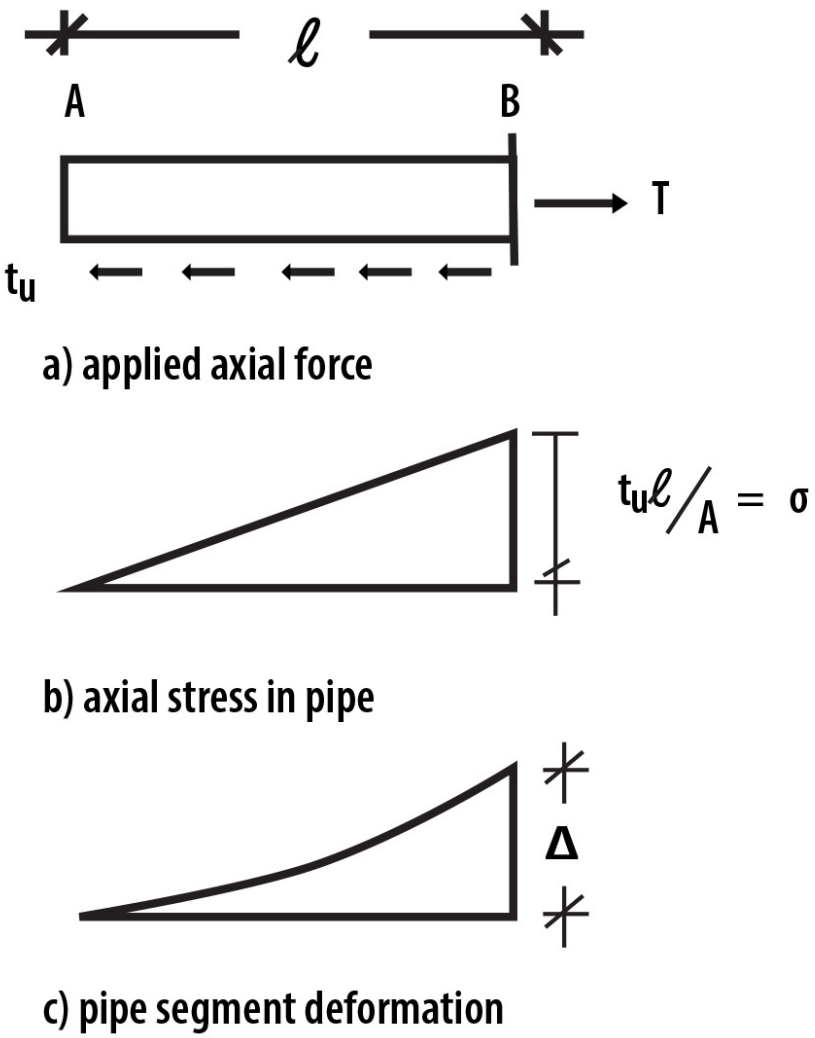

Figure A2 Applied Axial Force, Axial Stress and Deformation

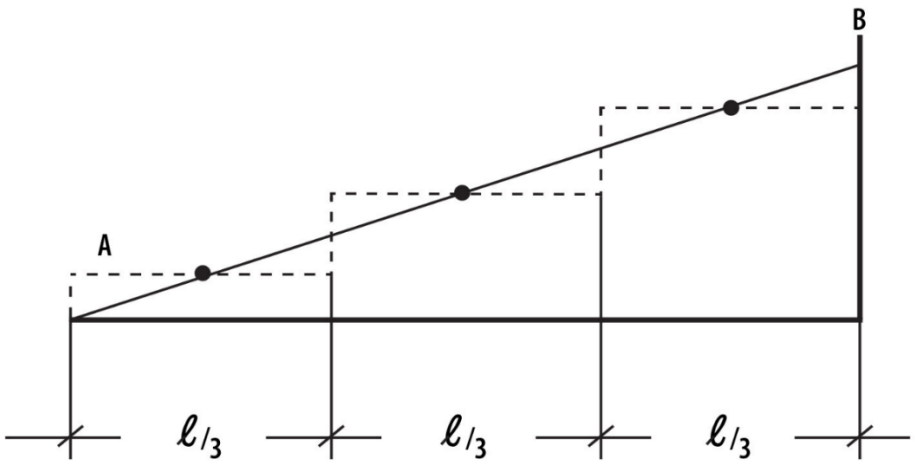

Figure A3 Subdivision of Pipe into Three Constant Modulus Sub-segments

For a generic i[th] sub region

$$\Delta_i = \int_{(i-1)l/n}^{il/n} \frac{t_u\, x}{AE_i} dx = \frac{t_u}{2AE_i} \left(\frac{l}{n}\right)^2 (2i-1)$$

Summing the contributions from the three sub regions in Figure A3, the pipe displacement at Point B is

$$\Delta = \sum_{i=1}^{3} \Delta_i = \frac{t_u l^2}{2A} \left(\frac{1}{3^2}\right) \left[\frac{1}{E_1} + \frac{3}{E_2} + \frac{5}{E_3}\right] \qquad \text{(A1)}$$

where for Case I, l = L/2, while for Case II l = L_e. As noted above, for Case II the ground displacement δ is twice the stretch over the region from Point A to B. Hence from Equation 15

$$\delta = 2\,\Delta = \frac{t_u\, L_e^2}{AE'}$$

and from Equation A1 above

$$\frac{t_u\, L_e^2}{AE'} = 2\,\frac{t_u\, L_e^2}{2A} \left(\frac{1}{9}\right) \left[\frac{1}{E_1} + \frac{3}{E_2} + \frac{5}{E_3}\right]$$

or the effective modulus E' (suitable for linearly increasing axial stress) is

$$\frac{1}{E'} = \frac{1}{9} \left(\frac{1}{E_1} + \frac{3}{E_2} + \frac{5}{E_3}\right) \qquad \text{(A2)}$$

The peak allowable axial strain for a HDPE pipe PE 4710 material subject to a lateral spread is likely in the 6% to 10% range. Herein we will calculate E´ for an axial strain of 8%.

Figure A1 shows the stress strain curve as well as stress and strain values at segment 1, 2 and 3 identified. Since, as noted above, the axial force and axial stress increase at a uniform rate (i.e., vary linearly) between zero stress at Point A to peak stress at Point B, the lengths of all three subsegments are the same. The axial stress and corresponding axial strain at the mid points of each of the three subsegments are listed in Table A2. The corresponding Elastic Modulus, E_i, assumed constant over the individual subsegments is also shown in Table A2. For example, at segment #2, E_2 = 2125 psi/0.0111 = 191,441 psi.

Table A2 Evaluation of E´ for 8% peak axial strain

Segment #	Stress (psi)	Strain	E_i (psi)
1	708	0.0266	266,165
2	2125	0.0111	191,441
3	3540	0.0335	105,671

The resulting effective modulus E´ for a peak axial strain of 8% is 134,860 psi using Equation A2. The corresponding effective modulus for peak axial stains of 6% and 10% are listed in Table A3.

Table A3 Effective Elastic Modulus E′ for Three Peak Axial Strain Values

Peak Axial Strain	Effective Modulus E′ (psi)
6%	145,650
8%	134,860
10%	127,460

Appendix B

Magnitude and Distance Map

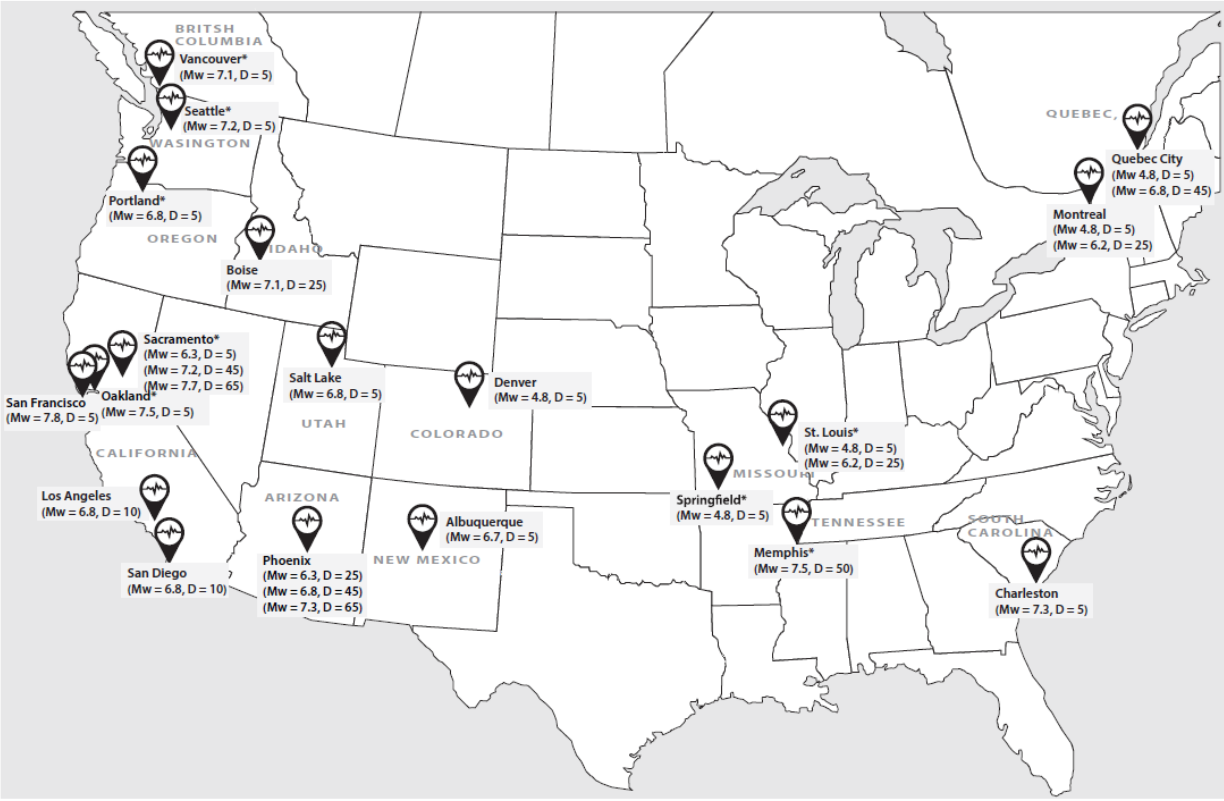

Figure B1: Earthquake Magnitude (Mw) and Closest Distance (D, Km) for Selected N. American Cities. For consistence with Figure 7, only Mw ≤ 8.0 and Distance ≤ 100km are considered. Astrix indicate contributing events above the Figure 7 limits.

LIST OF VARIABLES AND ABBREVIATIONS

A	Pipe Cross Sectional Area (in^2)
D	Pipe Diameter (in.)
$(D_{50})_{15}$	Average Mean Grain Size in T_{15}
E_i	HDPE Secant Elastic Modulus at a specific axial stress (specimen subject to uniform axial stress) (psi)
E'	Effective Elastic Modulus for a specific peak axial strain (specimen subject to linearly increasing axial stress) (psi)
F_{15}	Average Fines Content in T_{15}
H	Pipe Burial Depth (ground surface to pipe spring line) (ft.)
k_o	Earth Pressure Coefficient
l	Pipe length between point of zero axial load and maximum axial load
L	Horizontal Extent of Lateral Spread Zone (plan dimensions in direction of ground movements (ft.)
L_{min}	Minimum value of L for which response is Case II
L^*	Controlling Pipe Length Parameter from Flowchart (ft.)
M, M_w	Earthquake Magnitude
PGD	Abbreviation for Permanent Ground Deformation
R, R_{eg}	Horizontal Distance from Seismic Energy Zone (km)
T_{15}	Thickness of the Saturated Layer with Blow Count $(N_1)_{60} \leq 15$
t	Pipe Wall Thickness (in.)
t_u	Axial Friction Force per unit length at Soil/Pipe Interface
α	Ground Strain for Ridge Pattern of Lateral Spreading
γ	Unit Weight of Soil (pcf)
ε_{eq}, ε	Equivalent Ground Strain
δ	Peak Horizontal Ground Displacement within Lateral Spread Zone (ft.)
δ_{min}	Minimum Value of δ for which response is Case I
Δ	Horizontal Displacement of Pipe at head and Toe of the Lateral Spread Zone (ft.)
Δ_i	Pipe Axial Displacement over subsegment i
σ_{max}	Peak Pipe Axial Stress (psi)
μ	Friction Coefficient between Pipe and Soil

REFERENCES

Ambraseys, N., (1988), “Engineering Seismology” Earthquake Engr. and Structural Dynamics, Vol. 17, pp. 1-105.

Bartlett, S., and Youd, T., (1995) “Empirical Prediction of Liquefaction-Induced Lateral Spread” Journal of Geotechnical Engr., ASCE, Vol. 121, No. 4, pp. 316-329.

Davis, C., Wham, B., Toshima, T., and Hara, T., (2019) “Case Studies of Hazard Resilient Ductile Iron Pipes Subjected to Longitudinal Permanent Ground Movements” Proceedings of the 15th JWWA/WRF/CTWWA Water System Seismic Conference, Los Angeles CA, October.

Electric Power Research Institute (EPRI), (2008), “Tensile Testing of Cell Classification 445474C High Density Polyethylene Pipe Material.

Gemperline, M., and Rinehart, R., (2018), “Soil Pipe Friction Coefficients for Buried PE4710 Pipe”, Bureau of Reclamation.

Hamada, M., Yasuda, S., Isoyama, R., and Emoto, K., (1986), “Study of Liquefaction Induced Permanent Ground Displacements”, Association for Development of Earthquake Prediction, Japan, 87p.

Honegger, D.G., (1994), “Assessing Vulnerability of BC Gas Pipelines to Lateral Spread Hazards”, Proceedings of the Fifth U.S.-Japan Workshop on Earthquake Design of Lifeline Facilities and Countermeasures Against Soil Liquefaction, MCEER-94-0026, pp. 515-530.

Morimoto, K., and Miyajima, M., (2019) “Study of Behavior of Seismic Type Ductile Iron Pipes in Large Deformation of Liquefied Ground by Multiple Times of Earthquake” Proceedings on the 15th JWWA/WRF/CTWWA Water System Seismic Conference, Los Angeles CA, October.

Omuro, H., and Himono, T., (2018) “Polyethylene Pipeline Performance Against Earthquake” Proceedings of the 19th Plastic Pipe Conference, PPXIX, September.

O’Rourke, M., Filipou, E., and Uckan, E., (2015), “Towards Robust Fragility Relations for Buried Segments Pipe in Ground Strain Areas” Earthquake Spectra, Vol. 21, No. 3, pp. 1-20.

O’Rourke, M.J., and Nordberg, C., (1992), “Behavior of Buried Pipelines Subject to Permanent Ground Deformation”, Tenth World Conference on Earthquake Engineering, Madrid, Spain, Vol. 9, pp. 5411 -5416.

Youd, T. L., and Perkins, D.M., (1987), “Mapping of Liquefaction Severity Index”, Journal of Geotechnical Engineering, ASCE, Vol. 113, No. 11, pp.1374-1392.

Youd, T. L., Hansen, C., and Bartlett, S., (2002), “Revised Multilinear Regression Equations for Prediction of Lateral Spread Displacement”, Journal of Geotechnical and Geoenvironmental Engineering, ASCE, Vol. 128, No. 2, pp.1007-1017.